Observational Analysis of the Wind-Evaporation-SST Feedback over the Tropical Pacific Ocean

Jia-Lin Lin[1], Weiqing Han[2] and Xin Lin[3]

[1]Department of Geography, The Ohio State University, Columbus, OH
[2]Department of Atmospheric and Oceanic Sciences, University of Colorado, Boulder, CO
[3]NASA GSFC Global Modeling and Assimilation Office, Greenbelt, MD

Atmos. Sci. Lett., in press

Corresponding author address: Dr. Jia-Lin Lin
Department of Geography, The Ohio State University
1105 Derby Hall, 154 North Oval Mall, Columbus, OH 43210
Email: lin.789@osu.edu

Abstract

Theoretical studies suggested that the wind-evaporation-SST (WES) feedback plays an important role in maintaining the latitudinal asymmetry of the Intertropical Convergence Zone (ITCZ) in tropical Pacific Ocean. This study examines the geographical distribution of the strength of WES feedback over the tropical Pacific Ocean using multiple long-term observational datasets. The results show that the WES feedback is very weak over the eastern Pacific warm pool and stratocumulus regions, where the strongest latitudinal asymmetry of the ITCZ exists, suggesting that some other mechanisms are responsible for the asymmetry. To the west of 120W, the WES feedback has larger magnitude but is often statistically insignificant. This is because the air-sea humidity difference effect tends to offset the wind effect, which is a factor not considered in the original WES feedback theory.

1. Introduction

An important question for tropical mean climate is why the annual mean Intertropical Convergence Zone (ITCZ) is located north of the equator in the central Pacific, eastern Pacific and Atlantic Oceans, although the annual mean solar radiation is roughly symmetric about the equator and has its maximum on the equator. Previous theoretical studies suggested that ocean-atmosphere feedback plays an important role in maintaining this latitudinal asymmetry of tropical mean climate (see reviews by Xie 2005 and Chang et al. 2006). There are two major ocean-atmosphere feedback mechanisms: the wind-evaporation-SST (WES) feedback (Xie and Philander 1994; Xie 1996a) and the stratus-SST feedback (Philander et al. 1996; Ma et al. 1996; Yu and Mechoso 1999; Gordon et al. 2000; de Szoeke et al. 2006), which enhance the meridional asymmetry associated with the continental forcing in the eastern boundary (e.g. Xie 1996a; Xie and Saito 2001), seasonal solar forcing (e.g. Xie 1996b), and atmosphere's internal dynamics (e.g. Charney 1971; Holton 1971; Lindzen 1974; Waliser and Somerville 1994; Chao 2000; Liu and Xie 2002).

Xie and Philander (1994) proposed the WES feedback mechanism for breaking the equatorial symmetry set by solar radiation (see schematic in Fig. 4-5 of Xie 2005). Suppose that somehow the sea surface temperature (SST) north of the equator becomes slightly warmer than to the south. This north-south SST gradient will lead to north-south sea level pressure (SLP) gradient (Gill 1980; Lindzen and Nigam 1987), which in turn will drive southerly winds across the equator. The Coriolis force acts to turn these southerlies westward south and eastward north of the equator. Superimposed on the background easterly trade winds, the anomalous westerly winds north of the equator decrease surface wind speed and hence latent heat flux (LHF), while the anomalous easterly winds south of the equator increase surface wind speed and associated LHF. These changes in LHF amplify the initial interhemispheric SST difference, and thus provide a positive feedback to the latitudinal asymmetry. The existence of WES feedback over the tropical Atlantic Ocean has been confirmed by several observational studies (e.g. Hu and Huang 2006), but the existence of WES feedback in over the tropical Pacific Ocean has not been examined using observational data.

The purpose of this study is to analyze the spatial distribution of the strength of WES feedback over tropical Pacific Ocean using multiple long-term observational datasets. The datasets used are described in section 2. Results are presented in section 3. A summary and discussion are given in section 4.

2. Data

We use 21 years (1979-1999) of monthly datasets of SST, precipitation, surface winds and latent heat flux. For each variable, different datasets are used whenever possible in order to sample the uncertainties associated with measurement/retrieval /analysis. The datasets used include:

(1) SST from the Extended Reconstruction of SST (ERSST; Smith and Reynolds 2004) and the Met Office Hadley Centre's Sea Ice and SST (HADISST; Rayner et al. 2003), both with a horizontal resolution of 1 degree longitude by 1 degree latitude,

(2) precipitation from the Global Precipitation Climatology Project (GPCP) Version 2 data (Adler et al. 2003) and the CPC Merged Analysis of Precipitation (CMAP;

Xie and Arkin 1996), both with a horizontal resolution of 2.5 degree longitude by 2.5 degree latitude, and

(4) surface winds from the NCEP/NCAR reanalysis (Kalnay et al. 1996) and ECMWF 40-year reanalysis (ERA40; Gibson et al. 1997), both with a horizontal resolution of 2.5 degree longitude by 2.5 degree latitude.

surface latent heat flux from the OAFLUX dataset (Yu et al. 2004), with a horizontal resolution of 2.5 degree longitude by 2.5 degree latitude.

Because we are interested only in the large-scale features, all datasets are averaged to have a zonal resolution of 10 degrees longitude but the original meridional resolutions are kept. We further smooth the data zonally using 30-degree running mean. We also tried 50-degree running mean and the results are similar.

3. Results

Our analysis follows step-by-step the WES feedback loop as discussed in the introduction. Since we are interested in the effect of WES feedback on the Pacific ITCZ, the region of interest is between 15°S-15°N, within which the ITCZ is generally confined. First we look at how the interhemispheric SST difference affects the off-equatorial precipitation. Figure 1 shows the linear regression of monthly data for 5°N-15°N (solid and dotted lines) and 5°S-15°S (dashed and dash-dotted lines) averaged precipitation versus the interhemispheric SST difference (ΔSST), which is defined as the difference between the 5°N-15°N averaged SST and the 5°S-15°S averaged SST. The diamonds (for solid lines) and squares (for dashed lines) denote that the corresponding linear correlation is above the 95% confidence level. The results are statistically significant over almost all regions. Precipitation in the northern hemisphere (NH) increases with ΔSST increase in all regions, with a 1 ^{o}C increase in ΔSST generally leading to more than 1 mm/day increase in precipitation. On the contrary, precipitation in the southern hemisphere (SH) decreases with ΔSST increase in all regions, although the magnitude is smaller over the eastern Pacific, which may be related to the lack of deep convection in the stratocumulus cloud region.

Precipitation is the dominant term of vertically-integrated diabatic heating in the troposphere. Consistent with the amplifying (weakening) of heating in the NH (SH), the cross-equatorial meridional wind (Figure 2) is enhanced in all regions, with a magnitude of 0.5-1.3 m/s for 1 ^{o}C increase in ΔSST. The zonal distribution pattern of zonal wind anomaly (Figure 3) is quite similar to that of precipitation anomaly in both the NH and SH (Figure 1), with a 0.5-2 m/s enhancement of zonal wind in NH in almost all regions and a 0.5-2 m/s decrease of zonal wind in SH over western and central Pacific. The zonal wind anomaly is small in the SH of eastern Pacific, which is consistent with the lack of deep convection anomaly in the stratocumulus region. It is also relatively small in the NH eastern Pacific warm pool region, which may be caused by the influence of nearby landmass and the associated North American monsoon (e.g. Lin et al. 2008).

The existence of time-mean background zonal wind is a necessary condition for the WES feedback, and its direction determines the sign of the wind speed anomaly. If the time-mean u is easterly, an easterly (westerly) zonal wind anomaly will enhance (suppress) the wind speed. Figure 4 shows the annual mean zonal wind averaged between 5^{o}N-15^{o}N and between 5^{o}S-15^{o}S. The time-mean zonal wind is easterly in all regions. Consistent with the zonal wind anomaly (Figure 3) and time-mean zonal wind (Figure 4), wind speed decreases with ΔSST increase in the NH, but increases with ΔSST increase in the SH (Figure 5). Interestingly, the wind speed sensitivity to ΔSST is small for both hemispheres over the eastern Pacific, where the strongest latitudinal asymmetry of the ITCZ exists! This is consistent with the weak meridional wind (Figure 2) and zonal wind (Figure 3) responses in this region.

Figure 6 shows the resultant LHF anomaly, whose magnitude corresponds to the strength of the WES feedback. Figure 6 demonstrates two important points. First, the WES feedback is very weak to the east of 250E, where the strongest latitudinal asymmetry of ITCZ exists (with the eastern Pacific warm pool in the NH and stratocumulus region in the SH). The LHF anomaly in the SH even shows a decrease, which means a negative feedback to ΔSST! This is against the enhancement of wind speed in this region (Figure 5). Therefore, the WES feedback cannot explain the latitudinal asymmetry of ITCZ in this region.

Secondly, to the west of 250E, the WES feedback has larger magnitude, but interestingly it is often statistically insignificant in spite of the fact that the wind speed anomaly is always statistically significant (Figure 5). This suggests that some factors other than the wind speed are strongly affecting the LHF anomaly. The LHF can often be expressed as (e.g. Liu et al. 1979):

$$LHF = \rho\, Lv\, C_D\, (q_{surface} - q_{air})\, V \qquad (1)$$

where ρ is the surface air density, Lv is the latent heat of water vapor, C_D is the transfer coefficient for latent heat, $q_{surface}$ is the surface saturation humidity which is determined by SST, q_{air} is the surface air humidity, and V is the surface wind speed. Therefore, the LHF anomaly can be expressed as:

$$LHF' = \rho\ Lv\ C_D\ [(q_{surface} - q_{air})]\ V' + \rho\ Lv\ C_D\ (q'_{surface} - q'_{air})\ [V] + \text{higher order terms} \quad (2)$$

where brackets represent annual mean and primes represent anomaly.

The first term on the right-hand side of Eq. 2 represents the wind effect, while the second term represents the air-sea humidity difference effect. As discussed in the introduction, the original WES feedback theory only considered the first term. However, the SST changes can lead to significant changes in surface saturation humidity and thus changes in the air-sea humidity difference. This is confirmed by Figure 7. The SST increase in the NH leads to significant increase of air-sea humidity difference (Figure 7a), which enhances the LHF anomaly and tends to offset the effect of reduced wind speed (Figure 5). Similarly, the SST decrease in the SH results in significant decrease of air-sea humidity difference (Figure 7b), which weakens the LHF anomaly and tends to offset the effect of enhanced wind speed (Figure 5).

To assess quantitatively the relative magnitude of the first term and second term in Eq. 2, Figure 8 shows the annual mean (a) air-sea humidity difference and (b) surface wind speed. The annual mean air-sea humidity difference is about 5 g/kg over most of the tropical Pacific Ocean, while the annual mean surface wind speed ranges from 2-6.5 m/s. When the annual mean air-sea humidity difference is multiplied by the surface wind anomaly (Figure 5), the product is of the same order as the product between annual mean surface wind speed and air-sea humidity difference anomaly (Figure 7). This explains the lack of statistical significance in the LHF anomaly to the west to 250E, and the negative sign of LHF anomaly in the SH stratocumulus region (Figure 6). Therefore, air-sea humidity difference needs to be considered in the WES feedback mechanism.

4. Summary

Theoretical studies suggested that the WES feedback plays an important role in maintaining the latitudinal asymmetry of the ITCZ in tropical Pacific Ocean. This study examines the geographical distribution of the strength of WES feedback over the tropical Pacific Ocean using multiple long-term observational datasets. The results show that the WES feedback is very weak over the eastern Pacific warm pool and stratocumulus regions, where the strongest latitudinal asymmetry of the ITCZ exists. To the west of 120W, the WES feedback has larger magnitude but is often statistically insignificant. This is because the air-sea humidity difference effect tends to offset the wind effect, which is a factor not considered in the original WES feedback theory.

Because the significant latitudinal asymmetry in the eastern Pacific is the original motivation for the WES feedback theory, the observed very weak WES feedback over this region was a surprising result to us, although it may not seem so surprising when the reader followed step-by-step our analysis. Our results suggest that some other mechanisms are responsible for the latitudinal asymmetry in this region. As discussed in the introduction, the possible candidates include the SST-stratus feedback (Philander et al. 1996; Ma et al. 1996; Yu and Mechoso 1999; Gordon et al. 2000; de Szoeke et al. 2006), continental forcing in the eastern boundary (e.g. Xie 1996a; Xie and Saito 2001), seasonal solar forcing (e.g. Xie 1996b), atmosphere's internal dynamics (e.g. Charney 1971; Holton 1971; Lindzen 1974; Waliser and Somerville 1994; Chao 2000; and Liu and Xie 2002).

In addition to the above possible mechanisms, ocean dynamics may also contribute significantly to the latitudinal asymmetry in the eastern Pacific. Recently, Shinoda and

Lin (2008) investigated the factors controlling the SST over the southeastern Pacific using an ocean general circulation model. They found that upper ocean heat budget is dominated by contributions from dynamical processes (costal upwelling and advection) instead of surface heat fluxes. Further analyses are needed to examine these mechanisms using observational datasets.

Acknowledgements

This study was supported by the NASA Modeling, Analysis and Prediction (MAP) Program.

REFERENCES

Adler, R.F., G.J. Huffman, A. Chang, R. Ferraro, P. Xie, J. Janowiak, B. Rudolf, U. Schneider, S. Curtis, D. Bolvin, A. Gruber, J. Susskind, and P. Arkin, 2003: The Version 2 Global Precipitation Climatology Project (GPCP) Monthly Precipitation Analysis (1979-Present). J. Hydrometeor., 4,1147-1167.

Bacmeister, J. T., M. J. Suarez, and F. R. Robertson, 2006: Rain Reevaporation, Boundary Layer–Convection Interactions, and Pacific Rainfall Patterns in an AGCM. J. Atmos. Sci., 62, 3383-3403.

Chang, P., T. Yamagata, P. Schopf, S. K. Behera, J. Carton, W. S. Kessler, G. Meyers, T. Qu, F. Schott, S. Shetye, and S.-P. Xie, 2006: Climate Fluctuations of Tropical Coupled Systems—The Role of Ocean Dynamics. J. Climate, 19, 5122-5174.

Chao, W. C., 2000: Multiple equilibria of the ITCZ and the origin of monsoon onset. *J. Atmos. Sci.*, **57**, 641-652.

Charney, J. G. 1971: Tropical cyclogenesis and the formation of the intertropical convergence zone. In, Reid, W.H. (ed.). *Mathematical Problems of Geophysical Fluid Dynamics.* Providence, Rhode Island: American Mathematics Society.

de Szoeke, S.P., Y. Wang, S.-P. Xie, and T. Miyama, 2006: The effect of shallow cumulus convection on the eastern Pacific climate in a coupled model. *Geophys. Res. Lett*., 33, L17713, doi: 10.1029/2006GL026715.

Gibson, J. K., P. Kållberg, S. Uppala, A. Hernandez, A. Nomura, and E. Serrano, 1997: ERA description. ECMWF Reanalysis Project Report Series 1, 86 pp.

Gill, A. E., 1980: Some simple solutions for heat induced tropical circulation. Quart. J. Roy. Meteor. Soc., **106**, 447-462.

Gordon, C.T., A. Rosati, and R. Gudgel. 2000. Tropical sensitivity of a coupled model to specified ISCCP low clouds. *Journal of Climate* 13: 2239–2260.

Holton, J. R., J.M. Wallace, and J.A. Young, 1971: On Boundary Layer Dynamics and the ITCZ. *J. Atmos. Sci*., **28**, 275-280.

Hu, Z. Z., and B. Huang, 2006: Physical Processes Associated with the Tropical Atlantic SST Meridional Gradient. *J. Climate.,* **19**, 5500–5518.

Lin, J. L., B.E. Mapes, K.M. Weickmann, G.N. Kiladis, S.D. Schubert, M. J. Suarez, J. Bacmeister, and M.-I. Lee, 2008: North American monsoon and convectively coupled equatorial waves simulated by IPCC AR4 coupled GCMs. *J. Climate*, 21, 2919-2937.

Lindzen, R. S., 1974: Wave-CISK in the tropics. *J. Atmos. Sci.*, 31, 156-179.

Lindzen, R. S., and S. Nigam, 1987: On the role of sea-surface temperature gradients in forcing low-level winds and convergence in the tropics. J. Atmos. Sci., 44, 2440-2458.

Liu, W.T. and X. Xie, 2002: Double Intertropical Convergence Zones - a new look using scatterometer. *Geophys. Res. Lett*., 29(22), 2072, doi:10.1029/2002GL015431.

Liu, W. T., Kristina B. Katsaros, and Joost A. Businger, 1979: Bulk Parameterization of Air-Sea Exchanges of Heat and Water Vapor Including the Molecular Constraints at the Interface. J. Atmos. Sci., 36, 1722-1735.

Ma, C.-C., C. R. Mechoso, A. W. Robertson, and A. Arakawa, 1996: Peruvian stratus clouds and the tropical Pacific circulation: A coupled ocean–atmosphere GCM study. *J. Climate.,* **9**, 1635–1645.

Philander, S. G. H., D. Gu, D. Halpern, G. Lambert, N.-C. Lau, T. Li, and R. C. Pacanowski,1996: Why the ITCZ is mostly north of the equator. *J. Climate,* 9, 2958–2972.

Rayner, N. A.; Parker, D. E.; Horton, E. B.; Folland, C. K.; Alexander, L. V.; Rowell, D. P.; Kent, E. C.; Kaplan, A., 2003: Global analyses of sea surface temperature, sea ice, and night marine air temperature since the late nineteenth century J. Geophys. Res., 108, No. D14, 4407 10.1029/2002JD002670.

Shinoda, T., and J. L. Lin, 2008: Interannual variation of upper ocean under stratocumulus cloud decks in the southeast Pacific. *J. Climate*, submitted.

Smith, T.M., and R.W. Reynolds, 2004: Improved Extended Reconstruction of SST (1854-1997). *J. Climate*, 17, 2466-2477.

Waliser, D. E., and R. C. J. Somerville, 1994: The preferred latitudes of the intertropical convergence zone. Journal of the Atmospheric Sciences, 51, 1619-1639.

Xie, P., and P. A. Arkin, 1996: Global precipitation: a 17-year monthly analysis based on gauge observations, satellite estimates, and numerical model outputs. Bull. Amer. Meteor. Soc., 78, 2539-2558.

Xie, S.-P, 1996a: Westward propagation of latitudinal asymmetry in a coupled ocean-atmosphere model. *Journal of Atmospheric Science,* 53, 3236–3250.

Xie, S.-P., 1996b: Effects of seasonal solar forcing on latitudinal asymmetry of the ITCZ. J. Climate, 9, 2945-2950.

Xie, S.-P, 2005: The shape of continents, air-sea interaction, and the rising branch of the Hadley Circulation. In H.F. Diaz and R.S. Bradley (eds.), The Hadley Circulation: Present, Past and Future, 121–152. Kluwer Academic Publishers. Pdf file available at: http://iprc.soest.hawaii.edu/~xie/hadley4camera.pdf

Xie, S.-P., and S. G. H. Philander. 1994. A coupled ocean-atmosphere model of relevance to the ITCZ in the eastern Pacific. *Tellus* 46A, 340–350.

Xie, S.-P. and K. Saito, 2001: Formation and variability of a northerly ITCZ in a hybrid coupled AGCM: Continental forcing and ocean-atmospheric feedback. *J. Climate*, 14, 1262-1276.

Yu, J.-Y., and C. R. Mechoso, 1999: Links between annual variations of Peruvian stratocumulus clouds and of SST in the eastern equatorial Pacific. *J. Climate,* 12, 3305–3318.

Yu, L., R. A. Weller, and B. Sun, 2004: Improving latent and sensible heat flux estimates for the Atlantic Ocean (1988-1999) by a synthesis approach. *J. Climate*, 17, 373-393.

FIGURE CAPTIONS

Figure 1. Linear regression of monthly data for 5oN-15oN (solid line and dotted line) and 5oS-15oS (dashed line and dash-dotted line) averaged precipitation vs interhemispheric SST difference (ΔSST). The diamonds (for solid line), triangles (for dotted line), squares (for dashed line) and crosses (for dash-dotted line) denote that the corresponding linear correlation is above the 95% confidence level.

Figure 2. Same as Figure 1 but for 5oN-5oS averaged surface meridional wind vs ΔSST.

Figure 3. Same as Figure 1 but for surface zonal wind vs ΔSST.

Figure 4. Annual mean surface zonal wind averaged between 5oN-15oN (solid line and dotted line) and 5oS-15oS (dashed line and dash-dotted line).

Figure 5. Same as Figure 1 but for surface wind speed vs ΔSST.

Figure 6. Same as Figure 1 but for LHF vs ΔSST.

Figure 7. Linear regression versus interhemispheric SST difference (ΔSST) for (a) 5oN-15oN and (b) 5oS-15oS averaged surface saturation humidity (solid line), surface air humidity (dotted line) and sea-air humidity difference (dashed line). The diamonds (for solid lines), triangles (for dotted lines) and squares (for dashed lines) denote that the corresponding linear correlation is above the 95% confidence level.

Figure 8. Annual mean (a) air-sea humidity difference and (b) surface wind speed averaged between 5oN-15oN (solid lines) and 5oS-15oS (dashed lines).

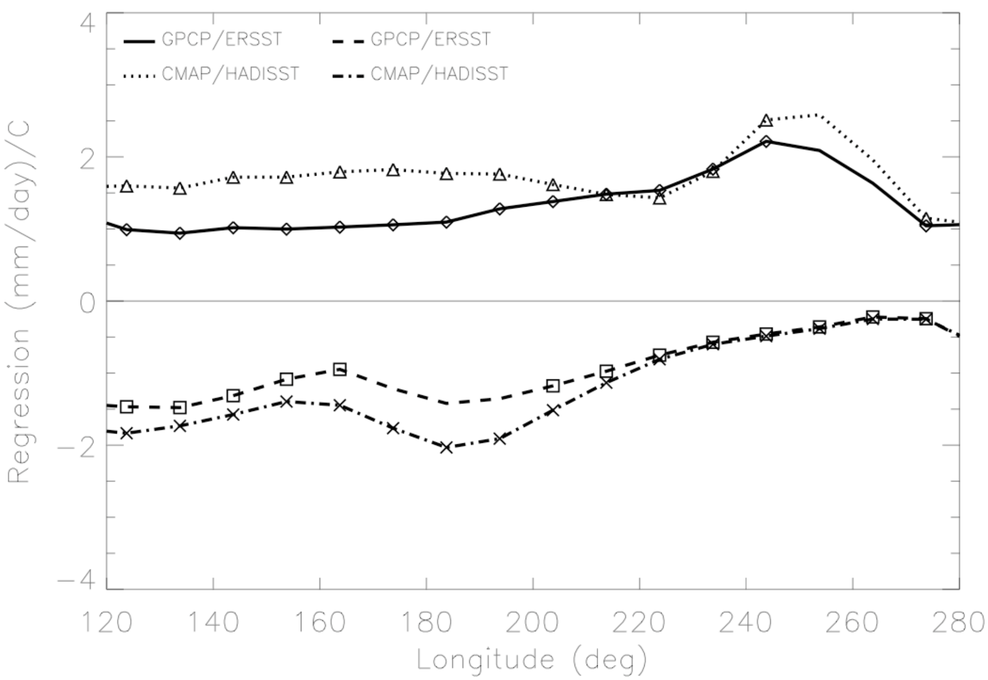

Figure 1. Linear regression of monthly data for 5°N-15°N (solid line and dotted line) and 5°S-15°S (dashed line and dash-dotted line) averaged precipitation vs interhemispheric SST difference (ΔSST). The diamonds (for solid line), triangles (for dotted line), squares (for dashed line) and crosses (for dash-dotted line) denote that the corresponding linear correlation is above the 95% confidence level.

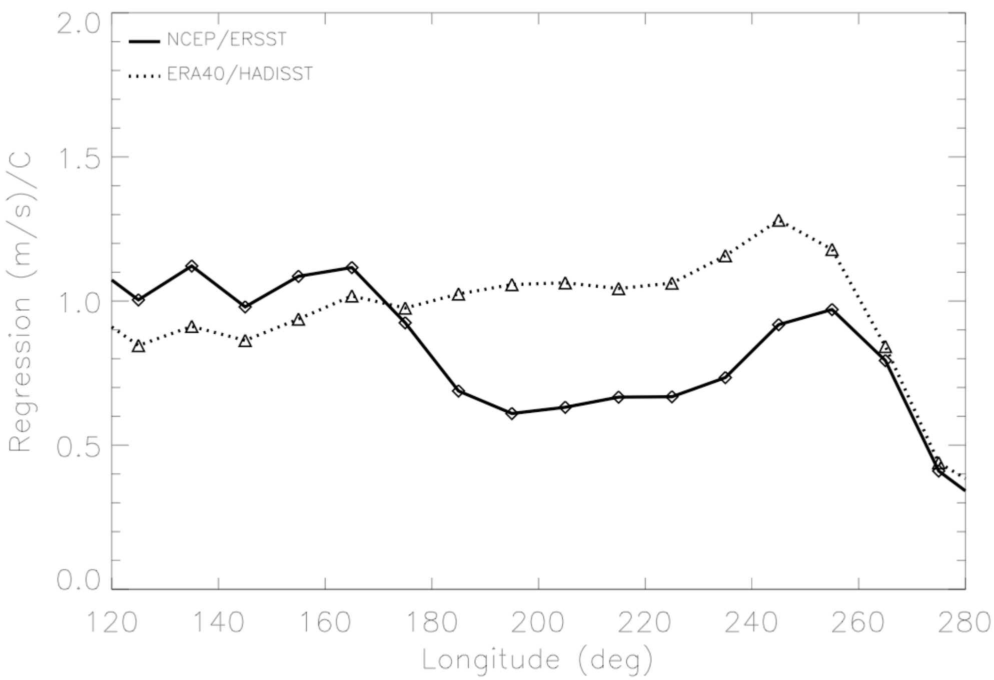

Figure 2. Same as Figure 1 but for 5^{o}N-5^{o}S averaged surface meridional wind vs ΔSST.

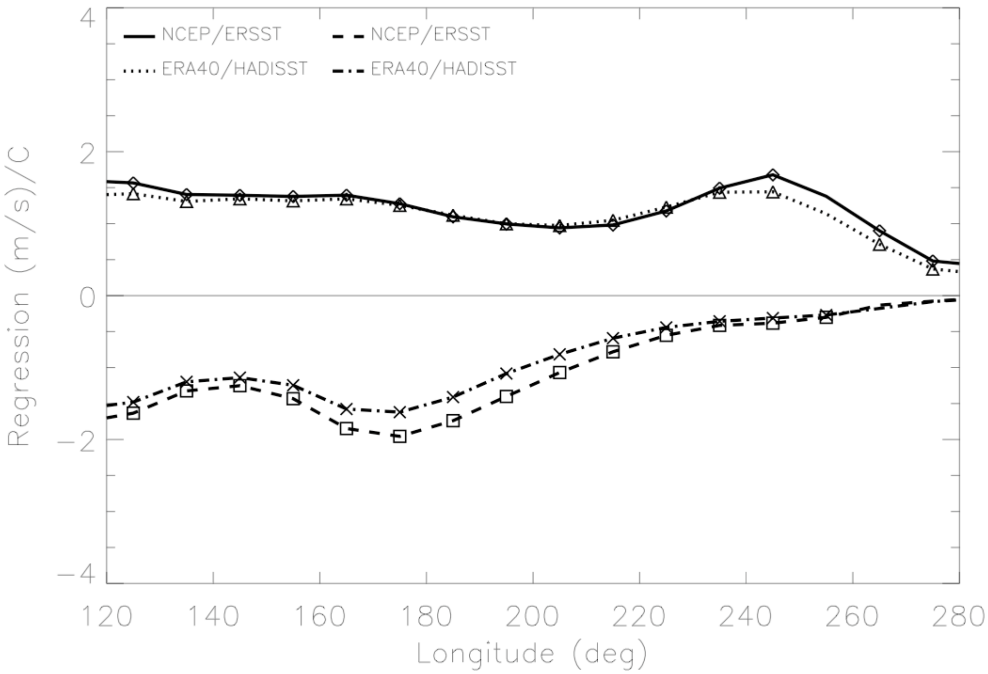

Figure 3. Same as Figure 1 but for surface zonal wind vs ΔSST.

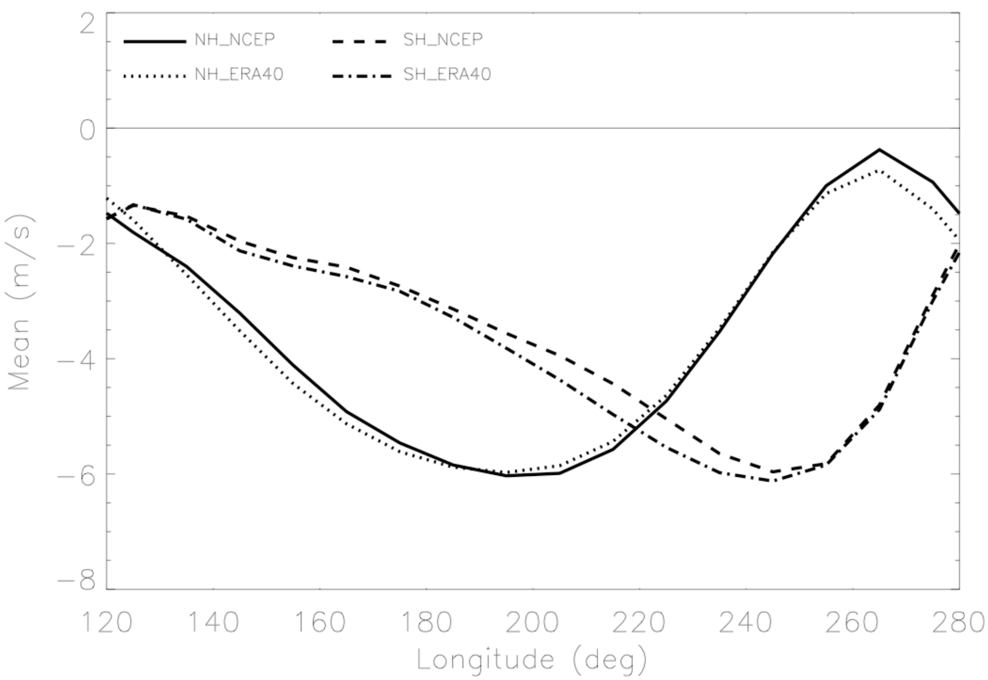

Figure 4. Annual mean surface zonal wind averaged between 5^{o}N-15^{o}N (solid line and dotted line) and 5^{o}S-15^{o}S (dashed line and dash-dotted line).

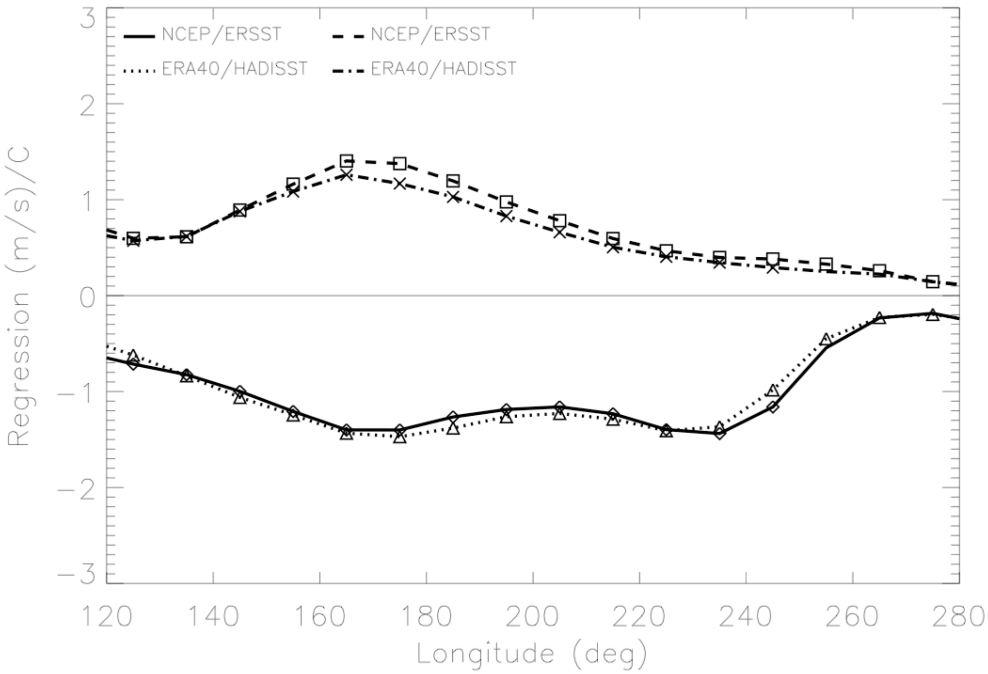

Figure 5. Same as Figure 1 but for surface wind speed vs ΔSST.

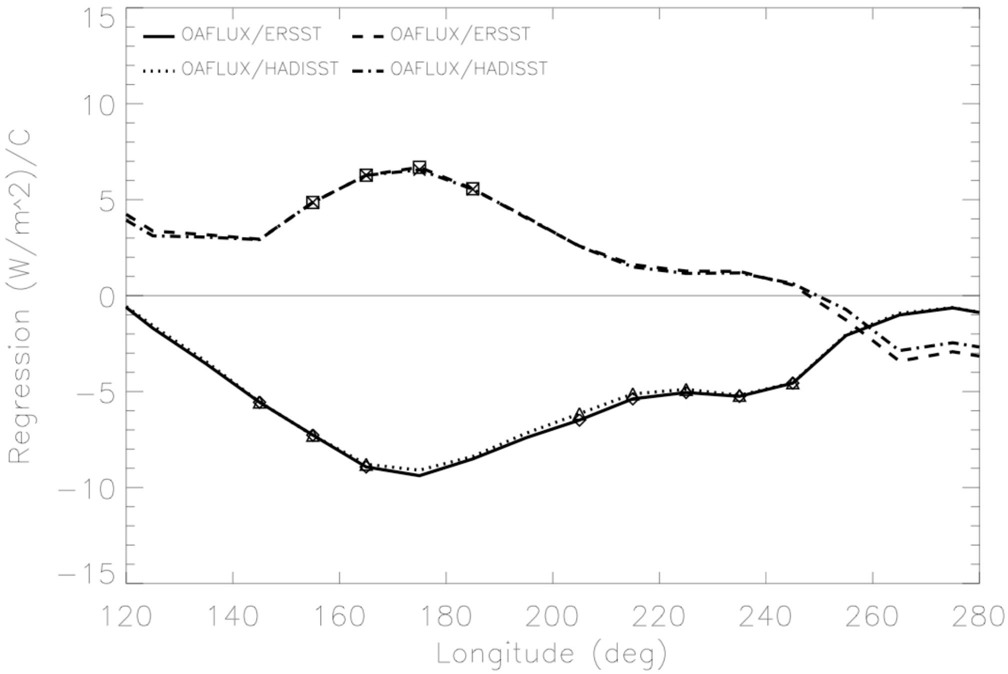

Figure 6. Same as Figure 1 but for LHF vs ΔSST.

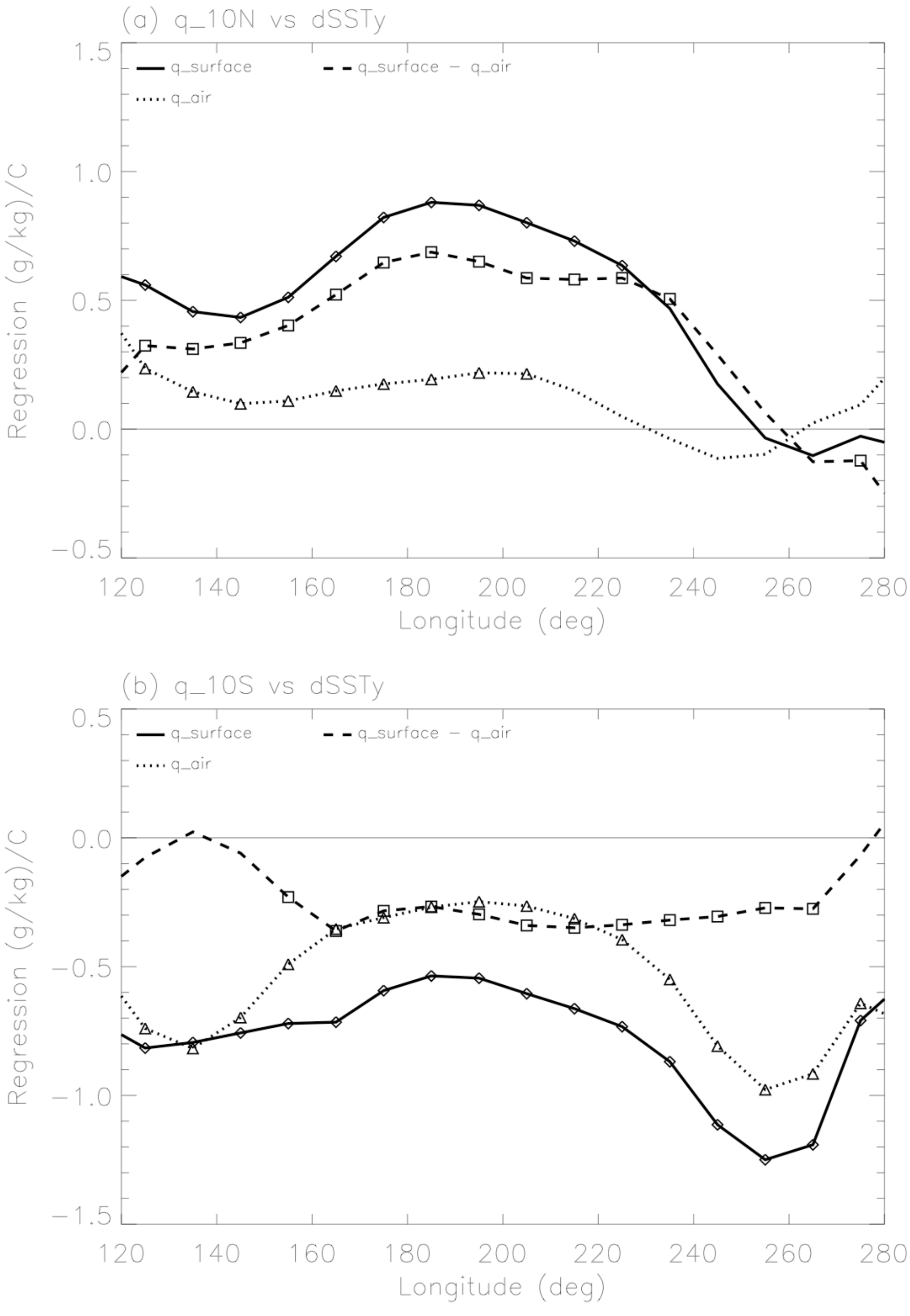

Figure 7. Linear regression versus interhemispheric SST difference (ΔSST) for (a) 5^{o}N-15^{o}N and (b) 5^{o}S-15^{o}S averaged surface saturation humidity (solid line), surface air humidity (dotted line) and sea-air humidity difference (dashed line). The diamonds (for solid lines), triangles (for dotted lines) and squares (for dashed lines) denote that the corresponding linear correlation is above the 95% confidence level.

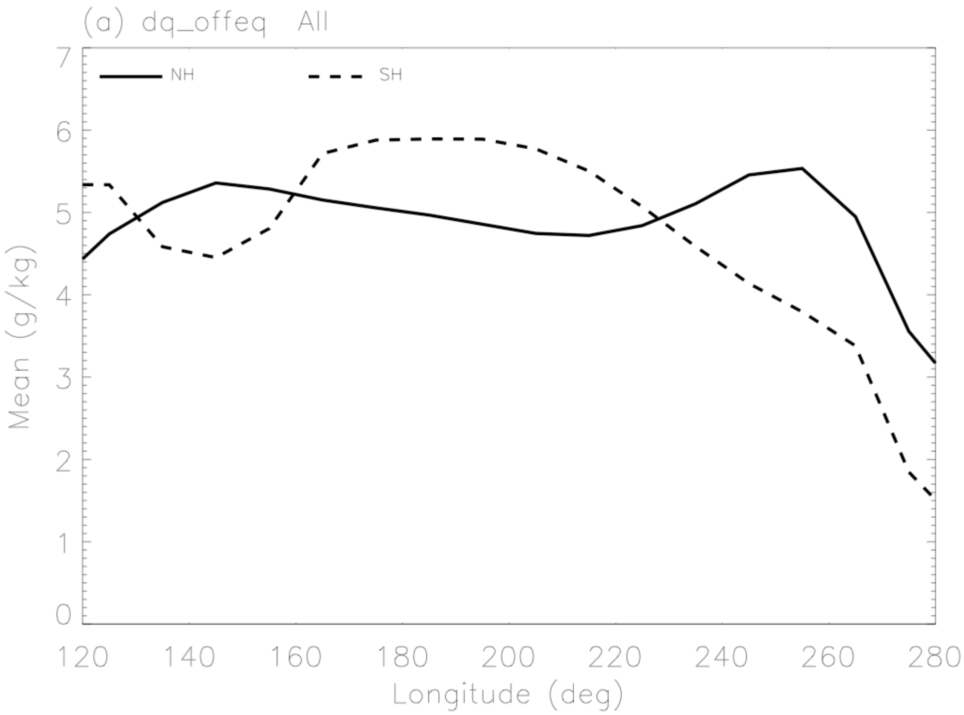

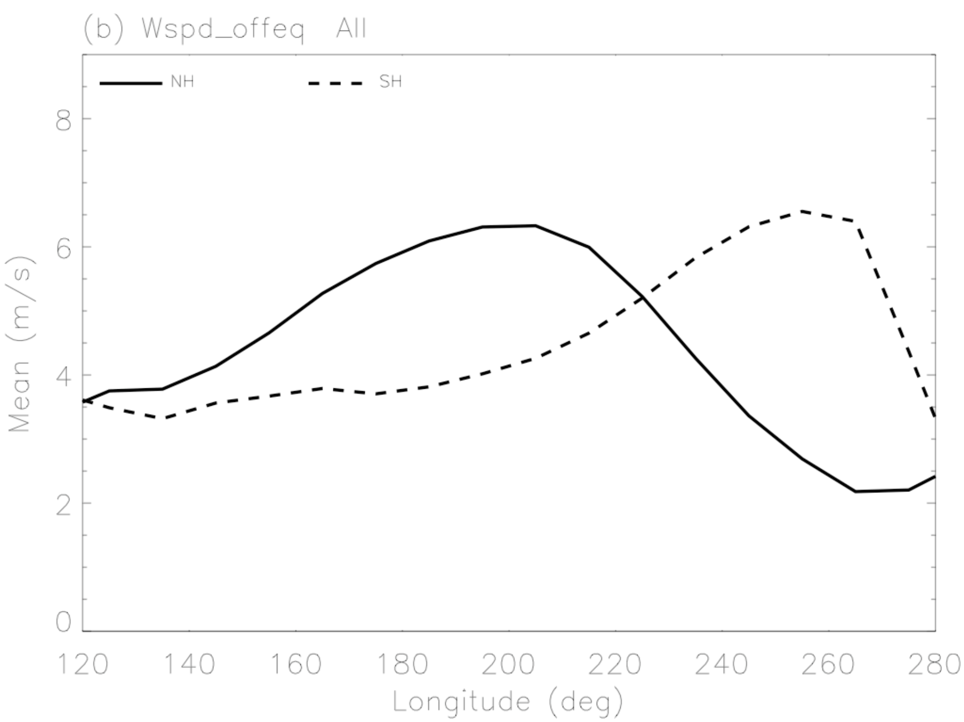

Figure 8. Annual mean (a) air-sea humidity difference and (b) surface wind speed averaged between 5^{o}N-15^{o}N (solid lines) and 5^{o}S-15^{o}S (dashed lines).